

Quantitative explanation of the magnetic resonance peak in high-temperature superconductors: Evidence for an extended s-wave pairing symmetry

Guo-meng Zhao

Department of Physics and Astronomy, California State University at Los Angeles, Los Angeles, CA 90032, USA

The microscopic pairing mechanism responsible for high-temperature superconductivity in copper-based perovskite oxides is still a subject of intense debate despite tremendous experimental and theoretical efforts for about 15 years. The debate has centered around the role of antiferromagnetic spin fluctuations in high-temperature superconductivity and the symmetry of superconducting condensate (order parameter). Extensive inelastic neutron scattering experiments have accumulated a great deal of important data that should be sufficient to address these central issues. Of particular interest is the magnetic resonance peak that has been observed in double-layer cuprate superconductors such as $\text{YBa}_2\text{Cu}_3\text{O}_{7-y}$ [1,6] and $\text{Bi}_2\text{Sr}_2\text{CaCu}_2\text{O}_{8+y}$ [7,8], and in a single-layer compound $\text{Tl}_2\text{Ba}_2\text{CuO}_{6+y}$ [9]. A number of theoretical models [10-15] have been proposed to explain the magnetic resonance peak, but none of them is able to account for all the experimental data in a consistent and quantitative way. Here we present quantitative explanations for the magnetic resonance peak and the spin gap in the neutron scattering data of cuprates by assuming that the order parameter has an extended s-wave (A_{1g}) symmetry and opposite signs in the bonding and antibonding electron bands formed within the Cu_2O_4 bilayers. In this picture, the neutron resonance peak is due to excitations of electrons from the extended saddle points below the Fermi level to the superconducting gap edge above the Fermi level. The A_{1g} pairing symmetry is compatible with a charge fluctuation mediated pairing mechanism [16].

The magnetic resonance peak observed in optimally doped and overdoped double-layer compounds $\text{YBa}_2\text{Cu}_3\text{O}_y$ (YBCO) [1,5] and $\text{Bi}_2\text{Sr}_2\text{CaCu}_2\text{O}_{8+y}$ (BSCCO) [7,8] is a sharp collective mode that occurs at an energy of 38-43 meV and at the two-dimensional wavevector $\vec{Q}_{AF} = (\pi, \pi)$, where π is the nearest-neighbor Cu-Cu distance. Fig. 1a shows the imaginary part of dynamical spin susceptibility as a function of excitation energy for an optimally doped double-layer compound $\text{YBa}_2\text{Cu}_3\text{O}_{6.92}$. The figure is reproduced from Ref. [5]. There are several striking features in the data: (a) The resonance peak at $E_r = 41$ meV appears below T_c and this resonance peak intensity $I^S(E_r)$ is larger than the normal-state intensity $I^N(E_r)$ by a factor of about 3.6, i.e., $I^S(E_r)/I^N(E_r) = 3.6$; (b) A spin gap feature is

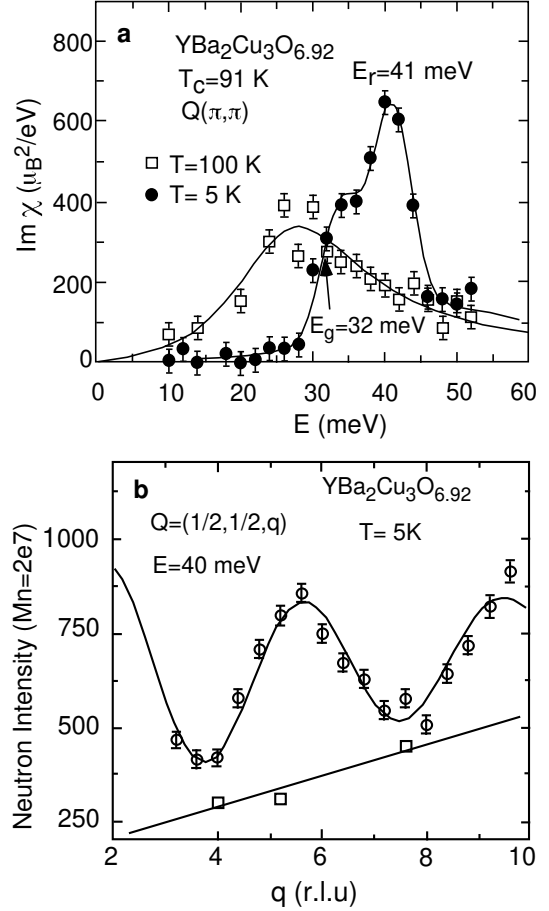


FIG. 1. a) The imaginary part of dynamical spin susceptibility as a function of excitation energy for $\text{YBa}_2\text{Cu}_3\text{O}_{6.92}$ in the normal and superconducting states. The figure was reproduced from Ref. [5]. b) q_1 -scan at $E = 40$ meV in $\text{YBa}_2\text{Cu}_3\text{O}_{6.92}$ displaying a modulation typical of odd excitation. The figure was reproduced from Ref. [4]. The background (lower line and open squares) was obtained from q -scans across the magnetic line. The upper solid curve is a fit to $a + bF^2(Q)\sin^2(\pi zq_1)$, where $F(Q)$ is the Cu magnetic form factor. The modulation is not complete as even excitations are sizable at $q_1 = 3.5, 7$ but with a magnitude 5 times smaller.

seen below T_c , and there is a small shoulder that occurs at an energy slightly above the spin gap energy $E_g = 32$ meV. Fig. 1b shows a q_1 -scan at $E = 40$ meV in $\text{YBa}_2\text{Cu}_3\text{O}_{6.92}$ displaying a modulation typical of odd excitation. The figure is reproduced from Ref. [4]. From Fig. 1b, we find feature (c): The interlayer scattering intensity within the Cu_2O_4 bilayers (odd channel) is larger

than the intralayer scattering intensity (even channel) by a factor of about 5, i.e., $I_{\text{odd}}^S(E) = I_{\text{even}}^S(E) = 5$ for $E = 40$ meV. From the neutron studies on different double-layer compounds with different doping levels, one finds feature (d): The resonance energy E_r does not increase with doping in the overdoped range but is proportional to T_c as $E_r = k_B T_c = 5.2$ in both underdoped and overdoped ranges [8].

On the other hand, the neutron data for an optimally doped single-layer compound $\text{Ti}_2\text{Ba}_2\text{CuO}_{6+y}$ (Tl-2201) are apparently different from those for double-layer compounds. This can be seen clearly from Fig. 2 where we plot the difference spectrum of the neutron intensities at $T = 27$ K ($< T_c$) and $T = 99$ K ($> T_c$), at a wavevector of $\vec{Q} = (0.5, 0.5, 12.25)$. The figure is reproduced from Ref. [9]. It is remarkable that the neutron intensity in the superconducting state is lower than in the normal state although a sharp peak feature is clearly seen at $E_r = 47$ meV. From the peak intensity of a Q scan along $\vec{Q} = (q, q, 12.25)$ at $E = 47.5$ meV (see Fig. 4 of Ref. [9]), the nonmagnetic background intensity is deduced (as indicated by the horizontal solid line) on the assumption that the nonmagnetic background intensity in the E scan is the same as that in the Q scan. With the knowledge of the nonmagnetic background contribution, we find that the resonance peak intensity $I^S(E_r)$ for the single-layer Tl-2201 is slightly lower than the normal-state intensity $I^N(E_r)$, i.e., $I^S(E_r)/I^N(E_r) = 0.87$. This is in sharp contrast with the above result for the double-layer compound $\text{YBa}_2\text{Cu}_3\text{O}_{6.92}$ where we found $I^S(E_r)/I^N(E_r) = 3.6$. Thus, we identify feature (e) as $I^S(E_r)/I^N(E_r) > 1$ for double-layer compounds and $I^S(E_r)/I^N(E_r) < 1$ for single-layer compounds.

Several theoretical models have been proposed to explain the magnetic resonance peak. In a more exotic approach [10], the neutron data are interpreted in terms of a collective mode in the particle-particle channel whose quantum numbers are spin 1 and charge 2. This model predicts that the resonance peak energy E_r is proportional to the doping level. Other models based on spin-fermion interactions also show that E_r increases monotonically with increasing p [11-13]. All these models have difficulty explaining feature (d): E_r does not increase with increasing p in the overdoped range. Further, all these models predict that $I^S(E_r)/I^N(E_r) > 1$, which is consistent with results for double-layer compounds, but in disagreement with the experimental data for the single-layer Tl-2201 (see Fig. 2). Alternatively, feature (d) observed in the double-layer compounds can be explained by a simple particle-hole excitation across d -wave superconducting gap within an itinerant magnetism model [2, 14]. This is because the particle-hole excitation energy increases with the superconducting gap which in turn should be proportional to T_c at least in the overdoped range. However, the feature $I^S(E_r)/I^N(E_r) < 1$

observed in the single-layer Tl-2201 cannot be explained in terms of d -wave symmetry because d -wave symmetry is only compatible with $I^S(E_r)/I^N(E_r) > 1$.

We can quantitatively explain all these neutron data [19] by assuming that the order parameter has an extended s -wave symmetry and opposite signs in the bonding and antibonding electron bands formed within Cu_2O_4 bilayers. In this picture, the neutron resonance peak is due to excitations of electrons from the extended saddle points below the Fermi level to the superconducting gap edge above the Fermi level.

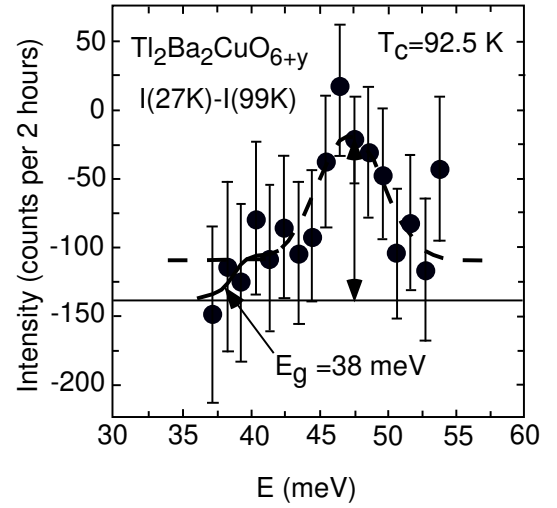


FIG. 2. The difference spectrum of the neutron intensities at $T = 27$ K ($< T_c$) and $T = 99$ K ($> T_c$), at wavevector $\vec{Q} = (0.5, 0.5, 12.25)$. The figure is reproduced from Ref. [9]. The dashed curve is the original data in Ref. [9] while the solid curve below 40 meV is a new fit, which is used to deduce the magnitude of the spin gap. The peak intensity of a Q scan along $\vec{Q} = (q, q, 12.25)$ at $E = 47.5$ meV (see Fig. 4 of Ref. [9]) is indicated by a vertical arrow. The nonmagnetic background intensity in the E scan is assumed to be the same as that in the Q scan and is indicated by the horizontal solid line.

It is known that the neutron scattering intensity at a wavevector \vec{q} and an energy E is proportional to the imaginary part of the dynamic electron spin susceptibility, $\chi''(\vec{q}; E)$. Qualitatively, with the neglect of the BCS (Bardeen, Cooper and Schrieffer) coherence factor, the bare imaginary part of spin susceptibility, $\chi''_0(\vec{q}; E)$, is proportional to the joint density of states $A(\vec{q}; E) = \sum_{\vec{k}} \delta(E - E_{\vec{k}+\vec{q}} - E_{\vec{k}})$, where $E_{\vec{k}} = \frac{\hbar^2 k^2}{2m}$ is the quasiparticle dispersion law below T_c , $\hbar k_F$ is the electronic band dispersion, and $\hbar k_F$ is the order parameter [15]. The two particle energy $E_2(\vec{k}; \vec{q}) = E_{\vec{k}+\vec{q}} + E_{\vec{k}}$ has a minimum and several saddle points for a fixed \vec{q} . The minimum defines the threshold energy, or spin gap energy E_g , which is achieved at vector \vec{k} and $\vec{k} + \vec{q}$ such that both \vec{k} and

$\mathbf{k} + \mathbf{q}$ belong to the Fermi surface and thus $E_g = 2 \epsilon_{\mathbf{k}}$ (Ref. [15]).

The joint density of states has a step at E_g and divergences at the extended saddle points [15]. The divergent peak in $\rho(\mathbf{q}; \omega)$ occurs because of transitions between the occupied states located in the extended saddle points below E_F and empty quasiparticle states at the superconducting gap edge above E_F . The saddle points produce Van Hove singularities in the quasiparticle density of states in the superconducting state at an energy of $\epsilon_{\mathbf{k}}^{\text{VH}} + \frac{2}{k}$ and the superconducting condensate creates a sharp coherence peak in the quasiparticle density of states at the gap edge. Thus, the divergence in the joint density of states in the superconducting state is then located at the energy $E = \epsilon_{\mathbf{k}+\mathbf{q}} + \epsilon_{\mathbf{k}}^{\text{VH}} + \frac{2}{k}$. This simple expression for E has been verified by numerical calculations in the case of an isotropic s-wave order parameter [15].

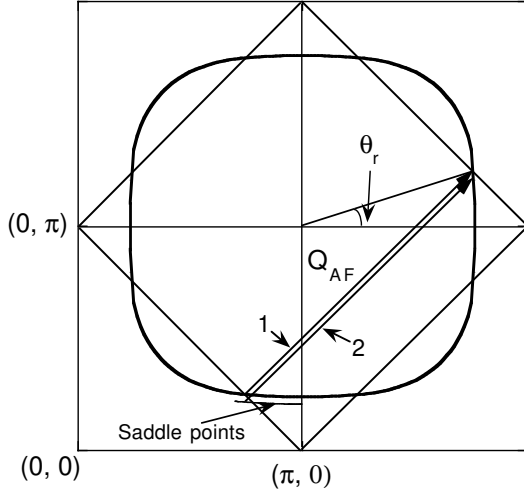


FIG. 3. The Fermi surface for a slightly underdoped BSCCO with $T_c = 88$ K. This Fermi surface is extrapolated from part of the Fermi surface determined by ARPES [17] using symmetry arguments. Arrow 1 indicates electron transitions from the occupied states in the superconducting gap edge below E_F to empty quasiparticle states at the gap edge above E_F . Arrow 2 marks electron transitions from the occupied states located in the extended saddle points below E_F to empty quasiparticle states in the superconducting gap edge above E_F .

In Fig. 3, we plot the Fermi surface for a slightly underdoped BSCCO, which is inferred by extending part of the Fermi surface determined by angle-resolved photoemission spectroscopy (ARPES) [17]. There are extended saddle points that are located near $(\pi, 0)$ and $(0, \pi)$; a portion of the extended saddle points are represented by a solid line in Fig. 3. If we only consider the magnetic excitations at a fixed wavevector that corresponds

to the antiferromagnetic wavevector Q_{AF} , only four electron wavevectors at the Fermi surface are connected by Q_{AF} as indicated by arrow 1 in Fig. 3. Each of these vectors forms an angle of $\pi/4$ with respect to the Cu-O bonding direction. The electron transitions from the occupied states located in the extended saddle points below E_F to empty quasiparticle states at the superconducting gap edge above E_F are indicated by arrow 2. Because the quasiparticle densities of states at the gap edge and the saddle points are divergent at zero temperature, such transitions will produce a sharp resonance peak at $E_r = \epsilon_{\mathbf{k}+Q_{AF}} + \epsilon_{\mathbf{k}}^{\text{VH}} + \frac{2}{k}$. In terms of $\pi/4$, both $E_g(Q_{AF})$ and $E_r(Q_{AF})$ can be rewritten as

$$E_g(Q_{AF}) = 2 \epsilon_{\pi/4} \quad (1)$$

and

$$E_r(Q_{AF}) = \epsilon_{\pi/4} + \frac{\epsilon_{\pi/4}^{\text{VH}}}{[\epsilon_{\pi/4}]^2 + (\frac{\text{VH}}{r})^2} \quad (2)$$

Here $\frac{\epsilon_{\pi/4}^{\text{VH}}}{[\epsilon_{\pi/4}]^2 + (\frac{\text{VH}}{r})^2}$ is the energy of a saddle point below the Fermi level along the $\pi/4$ direction. One should note that Eq. 2 is valid only if the saddle points are very close to the Fermi surface, as it is the case.

The above picture can explain the neutron resonance feature in the energy scan with a fixed Q_{AF} (see above). However, it cannot explain the neutron resonance feature in the Q scan at a fixed resonance energy because the observed peak is sharply located in Q_{AF} while this simple model predicts the existence of the peaks in other values of q if the order parameter is an isotropic s-wave [15]. This is because transitions from the occupied states located in the extended saddle points below E_F to empty sharp quasiparticle states at the superconducting gap edge above E_F are allowed for other values of q with nearly the same excitation energy in the case of isotropic s-wave. For an anisotropic s-wave, the peaks exist for other values of q but with different energies.

In order to understand the Q scan at a fixed resonance energy, one needs to consider the antiferromagnetic correlation between conduction electrons, which has been clearly seen in nuclear magnetic resonance studies [18]. In the presence of the antiferromagnetic correlation, the bare spin susceptibility is renormalized in a random phase approximation [19]. Since the antiferromagnetic interaction between the nearest neighbors acquires a peak at Q_{AF} , the renormalized spin susceptibility has a sharp maximum at Q_{AF} . In other words, because of the antiferromagnetic correlation, the dynamic spin susceptibility is greatly enhanced only near Q_{AF} so that the susceptibility for other wavevectors is negligibly small compared with the one near Q_{AF} . In light of this picture, one expects that the neutron intensities at fixed Q_{AF} in both normal and superconducting states should increase with decreasing doping because the antiferromagnetic correlation also

increases with decreasing doping. This is in agreement with experiment [4].

So far we have not considered the BCS coherence factor [20]:

$$(g_{\mathbf{k}}) = 1 - \frac{\mathbf{k} \cdot \mathbf{k} + \mathbf{q} + \mathbf{k} \cdot \mathbf{q}}{E_{\mathbf{k}} E_{\mathbf{k} + \mathbf{q}}} \quad (3)$$

For $\mathbf{k} \ll \mathbf{k} + \mathbf{q}$ and $\mathbf{k} + \mathbf{q} \ll \mathbf{k} + \mathbf{q}$, the BCS coherence factor is close to 2 when $\mathbf{k} + \mathbf{q}$ and \mathbf{k} have opposite signs, but is close to zero when $\mathbf{k} + \mathbf{q}$ and \mathbf{k} have the same sign. However, the coherence factor is not negligible for $\mathbf{k} \ll \mathbf{k}$ and $\mathbf{k} + \mathbf{q} = 0$ even if $\mathbf{k} + \mathbf{q}$ and \mathbf{k} have the same sign. More specifically, for excitation energies close to the resonance energy and for the excitations at Q_{AF} , the dominant contribution to the neutron intensity is the electron excitations from the states near the saddle points below the Fermi level to the superconducting gap edge above the Fermi level. This is because the quasiparticle density of states near the gap edge is divergent at zero temperature and because the density of states near the saddle points is large. Then the final states for electron excitations are limited to the states with $\mathbf{k} + Q_{AF} = 0$. By setting $\mathbf{k} + Q_{AF} = 0$ in Eq. 3, we find that

$$(E) = 1 - \frac{r}{E} = 1 - \frac{E_g}{2E} \quad (4)$$

where + corresponds to the case where $\mathbf{k} + Q_{AF}$ and \mathbf{k} have opposite signs and - to the case where $\mathbf{k} + Q_{AF}$ and \mathbf{k} have the same sign. It is apparent that for $E \ll E_g$, $+(E)$ is close to 2 while $-(E) \approx 0$. When E_r is significantly larger than E_g , both $+(E_r)$ and $-(E_r)$ are finite and $+(E_r) \gg -(E_r)$. Since the neutron intensity is proportional to the BCS coherence factor, one should see the magnetic resonance peak as long as the BCS coherence factor at the resonance energy is substantial. This is always the case when $\mathbf{k} + Q_{AF}$ and \mathbf{k} have opposite signs. This is also the case when $\mathbf{k} + Q_{AF}$ and \mathbf{k} have the same sign and E_r is significantly larger than E_g . The intensity of the resonance peak also depends on the band dispersion and the strength of the antiferromagnetic correlation. The failure to see the resonance peak may arise from disorders that smear Van Hove singularities and/or from the presence of more dispersive saddle points.

For a single-layer compound with d-wave order parameter symmetry, $\mathbf{k} + Q_{AF}$ and \mathbf{k} have opposite signs so that $+(E_r) \approx 2$ and thus $I^S(E_r)/I^N(E_r) \gg 1$. Therefore, the experimental observation of $I^S(E_r)/I^N(E_r) = 0.87 < 1$ in the single-layer Tl2201 [9] indicates that the order parameter in this single layer compound is not d-wave. Alternatively, for a single-layer compound with an s-wave symmetry, $\mathbf{k} + Q_{AF}$ and \mathbf{k} have the same sign and $-(E_r) < 1$. In this case, $I^S(E_r)$ could be smaller or larger than $I^N(E_r)$ depending on the value of $-(E_r)$ and

the sharpness of the resonance. Using $E_r = 47$ meV, $E_g = 38$ meV (see Fig. 2), and Eq. 4, we calculate $-(E_r) = 0.32$. The rather small value of $-(E_r)$ may make $I^S(E_r)/I^N(E_r) < 1$, in agreement with the experimental result [9]. Hence, only s-wave symmetry is compatible with the observed result: $I^S(E_r)/I^N(E_r) = 0.87$.

For a double-layer compound, interactions within Cu_2O_4 bilayers yield bonding and antibonding bands. Transitions between electronic states of the same type (bonding-to-bonding or antibonding-to-antibonding) and those of opposite types are characterized by even or odd symmetry, respectively, under exchange of two adjacent CuO_2 layers. As a result, the magnetic excitations between different layers correspond to odd channel while the excitations within the same layer to even channel [4]. If the order parameters in the bonding and antibonding bands have the same sign, the magnetic resonance intensities in both channels should be similar for either s-wave or d-wave symmetry within the same band. This is because the BCS coherence factors for both channels are the same in this case. On the other hand, if the order parameter has an s-wave symmetry and opposite signs in the bonding and antibonding electron bands, the magnetic resonance intensity in the odd channel will be much larger than that in the even channel due to the large difference in their BCS coherence factors. This is the only option that is consistent with the observed feature (c): $I_{\text{odd}}^S = I_{\text{even}}^S = 5$, provided that the optical magnon gap due to interlayer magnetic coupling is much smaller than the resonance energy, which should be the case (see discussion below).

The optical magnon gaps in optimally doped and overdoped YBCO are much smaller than the resonance energy of 40 meV. This can be clearly seen from the doping dependence of the optical magnon gap; the gap is about 50 meV for $\text{YBa}_2\text{Cu}_3\text{O}_{6.5}$ while the gap is reduced to 25 meV for $\text{YBa}_2\text{Cu}_3\text{O}_{6.7}$ (Ref [21]). If the optical magnon gap decreases linearly with the oxygen content, it will go to zero in $\text{YBa}_2\text{Cu}_3\text{O}_y$ for $y > 0.9$. Moreover, for the underdoped $\text{YBa}_2\text{Cu}_3\text{O}_{6.7}$, the even-channel magnetic intensity in the normal state is found to be slightly smaller than the odd-channel one for $E = 40$ meV (Ref [21]). This is understandable because the excitation energy of 40 meV is well above the optical magnon gap of 25 meV and because magnetic excitations are not reduced for excitation energies well above the magnon gap [21]. Since the optical magnon gaps for optimally doped and overdoped $\text{YBa}_2\text{Cu}_3\text{O}_y$ are diminished, it is natural that $I_{\text{odd}}^N(E) = I_{\text{even}}^N(E) \approx 1$ for $E \gg 40$ meV. Therefore, the observed feature (c): $I_{\text{odd}}^S(E_r) = I_{\text{even}}^S(E_r) \gg 1$ for optimally doped and overdoped YBCO can only be explained by an order parameter that has an s-wave symmetry and opposite signs in the bonding and antibonding electron bands.

Because the magnetic intensity is proportional to the

BCS coherence factor, the difference in the magnetic resonance intensities in the even and odd channels is due to the difference in their BCS coherence factors that are associated with the sign of the order parameter. This simple argument leads to a relation

$$\frac{I_{\text{odd}}^S(E)}{I_{\text{even}}^S(E)} = \frac{f_{\text{odd}}^S(E)}{f_{\text{even}}^S(E)}: \quad (5)$$

For the optimally doped $\text{YBa}_2\text{Cu}_3\text{O}_{6.92}$, the result in Fig. 1b shows that $I_{\text{odd}}^S(E) = I_{\text{even}}^S(E) = 5$ for $E = 40$ meV. By substituting $E = 40$ meV and $E_g = 32$ meV into Eqs. 4 and 5, we find $f_{\text{odd}}^S(E) = I_{\text{even}}^S(E) = 5$, in quantitative agreement with the experimental result. For the overdoped $\text{YBa}_2\text{Cu}_3\text{O}_{6.97}$, the neutron data show that $I_{\text{odd}}^S(E) = I_{\text{even}}^S(E) \approx 10$ for $E = 37$ meV (Ref. [3]). Substituting $E = 37$ meV and $E_g = 33$ meV (Ref. [3]) into Eqs. 4 and 5 yields $I_{\text{odd}}^S(E) = I_{\text{even}}^S(E) = 9.5$, in excellent agreement with the experimental result (≈ 10).

For the optimally doped $\text{YBa}_2\text{Cu}_3\text{O}_{6.92}$, we can also deduce the value of $I_{\text{even}}^S(E_r)/I_{\text{even}}^N(E_r)$ using the measured $I_{\text{odd}}^S(E_r)/I_{\text{odd}}^N(E_r) = 3.6$ and the fact that $I_{\text{odd}}^N(E_r) = I_{\text{even}}^N(E_r) \approx 1$ (see above discussion). From Eqs. 4 and 5, we obtain $I_{\text{even}}^S(E_r) = 0.22 I_{\text{odd}}^S(E_r)$ and thus $I_{\text{even}}^S(E_r) = I_{\text{even}}^N(E_r) = 0.22 I_{\text{odd}}^S(E_r) = I_{\text{odd}}^N(E_r) = 0.80$. This value is very close to that (0.87) measured for the single-layer T2201. These results consistently suggest that the intralayer neutron intensity at E_r in the superconducting state is slightly lower than that in the normal state. This is not consistent with d-wave order parameter symmetry because d-wave symmetry predicts that $I_{\text{even}}^S(E_r) = I_{\text{even}}^N(E_r) \gg 1$ for bilayer compounds and $I^S(E_r) = I^N(E_r) > 1$ for single-layer compounds.

From Eqs. 1 and 2, it is also easy to calculate E_g and E_r if one knows the gap function $\Delta(\mathbf{k})$ and the \mathbf{k}_r value. From the measured Fermi surface, one can readily determine \mathbf{k}_r . For example, we find $\mathbf{k}_r = 18.4^\circ$ for a slightly underdoped BSCCO from Fig. 3. For optimally doped cuprates, we get $\mathbf{k}_r \approx 16.0^\circ$. If we could use an isotropic s-wave gap function $\Delta(\mathbf{k}) = 28$ meV for a slightly overdoped YBCO, we would have $E_g = 56$ meV, which is far larger than the measured one (33 meV). If we could use a d-wave gap function $\Delta(\mathbf{k}) = 28 \cos 2\theta$ meV, we would have $E_g = 47.5$ meV, which is also far larger than the measured one. Therefore, neither isotropic s-wave nor d-wave symmetry can explain the spin gap observed in the slightly overdoped YBCO.

Alternatively, an extended s-wave with eight line nodes (A_{1g} symmetry) is in quantitative agreement with two-third experiments that were designed to test the order-parameter symmetry for hole-doped cuprates [22]. The remaining one-third experiments (e.g., Tricrystal grain-boundary Josephson junction experiments) were explained qualitatively by Zhao [22] and by Brandow [23]. For a slightly overdoped YBCO, more than six independent experiments consistently suggest that [22] the gap

function is $\Delta(\mathbf{k}) = 24.5(\cos 4\theta + 0.225)$ meV. Substituting $\mathbf{k}_r = 16^\circ$ into the gap function, we get $\Delta(\mathbf{k}_r) = 16.3$ meV and thus $E_g = 32.6$ meV, in quantitative agreement with the measured one (32-33 meV).

In our model, the position of the extended saddle point along the \mathbf{k}_r direction is located at $E_r - E_g = 2$ in the superconducting state (see Eqs. 1 and 2). For the optimally doped YBCO with $E_r = 41$ meV and $E_g = 32$ meV, we

find that the saddle point in the superconducting state is located at an energy of 25 meV below the Fermi level. This is in agreement with the ARPES studies [24] which suggest that the Fermi level in the superconducting state for optimally doped cuprates is 30 meV above the extended saddle points that have the same energy over a large momentum space. Further, electronic Raman scattering spectra in $\text{YBa}_2\text{Cu}_4\text{O}_8$ have been used to determine the energy of the extended saddle points more accurately [25]. At 10 K (well below T_c), the energy of the extended saddle points is found to be 24.3 meV below the Fermi level, in excellent agreement with that (≈ 25 meV) deduced from the neutron data.

The A_g (extended s-wave) pairing symmetry was proposed early by Littlewood and coworkers [16]. Based on a three band Hubbard model, they showed that undamped charge fluctuations between Cu and O could induce electron pairing with A_g symmetry [16]. The energy of the fluctuations is about 2 eV. Indeed, a strong coupling between high-energy electronic excitations (≈ 2 eV) and conduction electrons has been clearly demonstrated by precise optical experiments [26]. This electronic coupling along with strong electron-phonon coupling leads to superconductivity with a transition temperature higher than 100 K [26,27]. Phenomenologically, the A_g pairing symmetry is also consistent with a pairing potential that has onsite repulsion and predominantly next nearest neighbor attraction [28].

Correspondence should be addressed to gzhao2@calstatela.edu

-
- [1] P. Bourges, Y. Sidis, B. Hennion, R. Villeneuve, G. Collin, and J. F. Manucco, *Physica B*, 213-214, 48 (1995).
 - [2] H. F. Fong, B. Keimer, P. W. Anderson, D. Reznik, F. Dogan, and I. A. Aksay, *Phys. Rev. Lett.* 75, 316 (1995).
 - [3] P. Bourges, L. P. Regnault, Y. Sidis, and C. Vettier, *Phys. Rev. B* 53, 876 (1996).
 - [4] Ph. Bourges, *The gap Symmetry and Fluctuations in High Temperature Superconductors*, Edited by J. Bok, G. deutscher, D. Pavuna and S. A. Wolf. (Plenum Press, 1998) p 349-371 (Vol. 371 in NATO ASI series, Physics).

- [5] Ph. Bourges, Y. Sidis, H. F. Fong, B. Keimer, L. P. Regnault, J. Bossy, A. S. Ivanov, D. L. Milius, I. A. Aksay, High Temperature Superconductivity, Edited by S. E. Barnes et al p207-212 (CP 483 American Institute of Physics, Amsterdam, 1999)
- [6] P. C. Dai, H. A. Mook, R. D. Hunt, and F. Dogan, Phys. Rev. B 63, 054525 (2001).
- [7] H. F. Fong, P. Bourges, Y. Sidis, L. P. Regnault, A. Ivanov, G. D. Guk, N. Koshizuka, and B. Keimer, Nature (London) 398, 588 (1999).
- [8] H. He, Y. Sidis, P. Bourges, G. D. Gu, A. Ivanov, N. Koshizuka, B. Liang, C. T. Lin, L. P. Regnault, E. Schoenher, and B. Keimer, Phys. Rev. Lett. 86, 1610 (2001)
- [9] H. He, P. Bourges, Y. Sidis, C. Ulrich, L. P. Regnault, S. Pailhes, N. S. Berzigiarova, N. N. Kolesnikov, B. Keimer Science 295, 1045 (2002).
- [10] E. Demler, and S. C. Zhang, Phys. Rev. Lett. 75, 4126 (1995). E. Demler, H. Kohno, and S. C. Zhang, Phys. Rev. B 58, 5719 (1998).
- [11] A. Abanov and A. V. Chubukov, Phys. Rev. Lett. 83, 1652 (1999).
- [12] D. K. Morr and D. Pines, Phys. Rev. Lett. 81, 1086 (1998).
- [13] J. Brinkmann and P. A. Lee, Phys. Rev. Lett. 82, 2915 (1999).
- [14] L. Yin, S. Chakravarty, and P. W. Anderson, Phys. Rev. Lett. 78, 3559 (1997); A. A. Abrikosov, Phys. Rev. B 57, 8656 (1998).
- [15] I. I. Mazin, Phys. Rev. Lett. 70, 3999 (1993).
- [16] P. B. Littlewood, C. M. Varma, and E. Abrahams, Phys. Rev. Lett. 63, 2602 (1989); P. B. Littlewood, Phys. Rev. B 42, 10075 (1990).
- [17] P. J. White, Z.-X. Shen, C. Kim, J. M. Harris, A. G. Loeser, P. Fournier, and A. Kapitulnik, Phys. Rev. B 54, R15 669 (1996).
- [18] N. J. Curro, T. Imai, C. P. Slichter, B. Dabrowski, Phys. Rev. B 56, 877 (1997).
- [19] M. U. Ubbens and P. A. Lee, Phys. Rev. B 50, 438 (1994).
- [20] J. R. Schrieffer, Theory of Superconductivity, (Frontiers in Physics (20), Addison Wesley, 1988).
- [21] H. F. Fong, P. Bourges, Y. Sidis, L. P. Regnault, J. Bossy, A. Ivanov, D. L. Milius, I. A. Aksay, B. Keimer Phys. Rev. B 61, 14773 (2000).
- [22] G. M. Zhao, Phys. Rev. B 64, 024503 (2001).
- [23] B. H. Brandow, Phys. Rev. B 65, 054503 (2002).
- [24] D. M. King, Z.-X. Shen, D. S. Dessau, D. S. Marshall, C. H. Park, W. E. Spicer, J. L. Peng, Z. Y. Li, and R. L. Greene, Phys. Rev. Lett. 73, 3298 (1994).
- [25] E. Ya. Sherman and O. V. Misochko, Phys. Rev. B 59, 195 (1999).
- [26] M. J. Holcomb, C. L. Perry, J. P. Coleman, and W. A. Little, Phys. Rev. B 53, 6734 (1996).
- [27] G. M. Zhao, V. Kirtikar, and D. E. Morris, Phys. Rev. B 64, 220506R (2001).
- [28] R. Fehrenbacher and M. R. Norman, Phys. Rev. Lett. 74, 3884 (1995).